Editors' Suggestion

Noise-Induced Backscattering in a Quantum Spin Hall Edge

Jukka I. Väyrynen,[1] Dmitry I. Pikulin,[1] and Jason Alicea[2,3]
[1]*Station Q, Microsoft Research, Santa Barbara, California 93106-6105, USA*
[2]*Department of Physics and Institute for Quantum Information and Matter, California Institute of Technology, Pasadena, California 91125, USA*
[3]*Walter Burke Institute for Theoretical Physics, California Institute of Technology, Pasadena, California 91125, USA*

(Received 31 May 2018; published 6 September 2018)

Time-reversal symmetry suppresses electron backscattering in a quantum-spin-Hall edge, yielding quantized conductance at zero temperature. Understanding the dominant corrections in finite-temperature experiments remains an unsettled issue. We study a novel mechanism for conductance suppression: backscattering caused by incoherent electromagnetic noise. Specifically, we show that an electric potential fluctuating randomly in time can backscatter electrons inelastically without constraints faced by electron-electron interactions. We quantify noise-induced corrections to the dc conductance in various regimes and propose an experiment to test this scenario.

DOI: 10.1103/PhysRevLett.121.106601

Introduction.—From a technological perspective, the main promise of two-dimensional topological insulators (2D TIs) stems from their edge states, which are protected by a combination of symmetry and topology [1–3]. The "helical" low-energy edge spectrum consists of *degenerate* counterpropagating electron states with opposite spins as required by time-reversal symmetry. Kramers orthogonality of the two states prevents elastic backscattering by a static potential, in turn yielding a quantized zero-temperature conductance $G = G_0 \equiv e^2/h$ per edge. Perfect quantization has, however, so far eluded experimental observation [4–12].

In practice, it was realized early on that many *inelastic* effects circumvent band-topology constraints and can hinder the edge-mode propagation by introducing backscattering [13–24]. These backscattering mechanisms reflect the fact that time-reversal symmetry allows *nondegenerate* counterpropagating states to have overlapping spin wave functions. Such nonzero overlap occurs generically in systems with fully broken spin-rotation symmetry. Indeed, it is well known that structural or bulk inversion asymmetry in 2D TIs may induce a nontrivial edge spin texture in momentum space [18]; that is, the edge-state spin quantization axis "rotates" as a function of momentum [25] as sketched in Fig. 1(a). The necessary energy transfer for backscattering was considered to originate from thermal itinerant edge electrons, or phonons, or fluctuating localized spins. Apart from the latter, the backscattering rate was found to be strongly suppressed at low temperatures: Electron-electron interactions perturbatively produce a conductance correction $\delta G \equiv G_0 - G \propto T^4$ at low temperatures [18,23,28], while phonon scattering is even more suppressed. Localized spins [29] impart a stronger effect in the perturbative limit $\delta G \propto \ln^2 T$, but their presence need not be a universal feature of all 2D TI materials.

In this paper, we show that a time-dependent scalar potential might dominate the backscattering in practice. This mechanism is expected to be ever-present in all materials in the form of electrical noise and is almost free from phase-space constraints.

We start from a qualitative derivation of our main result, the estimate of the decrease δG in the edge dc conductance. Spin texture in momentum space makes the edge electron density operator off diagonal in the basis of right and left movers [26]. Coupling the total density to a scalar potential $U(x)$ thus produces an effective backscattering matrix element $V_{pR\to p'L}$ that, for small energy transfer $v|p+p'|$, vanishes as $V_{pR\to p'L} = (v/D)(p+p')U_{2k_F}$. (We use $\hbar = k_B = 1$ units.) Here p, p' are momenta

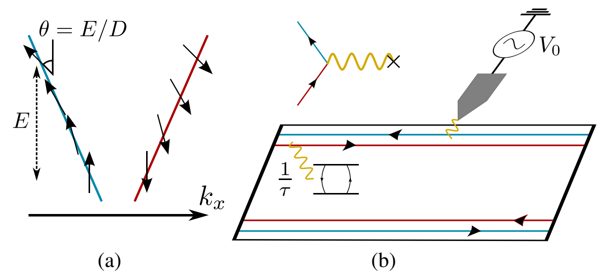

FIG. 1. (a) Spin texture in momentum space. Over a small energy interval E, the spin of an eigenstate rotates by a small angle E/D. (b) A time-dependent scalar potential induces backscattering when such spin textures exist. The potential can arise from a fluctuating two-level system near the edge or from an ac voltage $\sim \cos \omega_0 t$ applied by a nearby gate; Eqs. (11) and (14) predict the respective decrease in two-terminal dc conductance arising from these sources. Note that an applied ac voltage provides a controlled way of probing the spin texture required in our scenario.

measured from the Fermi points $\pm k_F$, and U_{2k_F} is the $2k_F$ Fourier component of the potential; v is the edge mode velocity, and D/v is the momentum scale over which the spin rotates; see Fig. 1(a). For a potential U fluctuating harmonically with frequency ω, the backscattering rate is $\Gamma = 2\pi\nu(\omega^2/D^2)|U_{2k_F}|^2$, where $\nu = 1/2\pi v$ is the edge density of states per length. When a bias voltage V is applied across the edge, νeV states contribute to the current. The backscattered current at low temperature thus reads $\delta I_\omega = 2\pi e^2\nu^2(\omega^2/D^2)|U_{2k_F}|^2 V$. One needs to integrate δI_ω over the full noise spectrum. A thermal noise source at temperature T can only emit photons of frequencies $\omega \lesssim T$, which cuts off the integration over ω. For low-frequency ($\omega \ll T$) noise caused by a single fluctuating electric dipole, modeled as a two-level system (TLS) with relaxation rate $\tau^{-1} \ll T$, the noise spectrum is Lorentzian, and the integration yields

$$\delta G \sim G_0 \frac{T|U_{2k_F}|^2}{D^2\tau v^2}, \tag{1}$$

which is one of our main results. The refined version of this equation appears in Eq. (11). On a long edge, many dipoles contribute incoherently to δG, leading to resistive edge transport. The long-edge resistance is obtained by summing Eq. (1) over impurities and averaging over τ. Assuming a distribution of relaxation times $P(\tau) \sim 1/\tau$ and a short-time cutoff τ_0, the resistance becomes

$$R \sim LnG_0^{-1} \frac{T|U_{2k_F}|^2}{D^2\tau_0 v^2}, \tag{2}$$

with L the length of the edge and n the number of dipoles per length. Equations (1) and (2) are valid at "high" temperatures where the dipoles are not frozen. In this regime, the mechanism does not lead to strong temperature dependence of R, unlike conventional backscattering processes arising, e.g., from electron-electron interactions on the edge.

Model and derivation.—The Hamiltonian of a clean helical edge is [18]

$$H_0 = \int \frac{dk}{2\pi} (\varepsilon_k c_{kR}^\dagger c_{kR} + \varepsilon_{-k} c_{kL}^\dagger c_{kL}), \tag{3}$$

with $\varepsilon_k = vk - \mu$ the spectrum linearized about the chemical potential $\mu = vk_F$. We stress that H_0 does not assume spin conservation and allows for a spin texture in momentum space. The spin of an eigenstate follows from the unitary transformation

$$\begin{pmatrix} c_{k\uparrow} \\ c_{k\downarrow} \end{pmatrix} = B_k \begin{pmatrix} c_{kR} \\ c_{kL} \end{pmatrix} \tag{4}$$

that relates fermions with spin $\uparrow, \downarrow$ to left and right movers. Unitarity and time-reversal symmetry impose $B_k^\dagger = B_k^{-1}$ and $B_k = B_{-k}$.

Consider next a time-dependent scalar potential that couples to the edge electron density $\rho = \sum_{\sigma=\uparrow,\downarrow} \psi_\sigma^\dagger \psi_\sigma$:

$$H_U(t) = \int dx \rho(x) U(x) w(t). \tag{5}$$

We assume here that the noise-induced potential has separable dependence on position and time, parametrized by $U(x)$ and $w(t)$, respectively. This assumption certainly holds for telegraph noise (two-level-system noise) from a single impurity, which we consider later. In the presence of $H_U(t)$, time-reversal symmetry is clearly broken but is maintained in a time-averaged sense.

Using Eq. (4) to express the density ρ in the L/R basis, we see that H_U does not conserve the number of left and right movers. In momentum space, the off-diagonal part of Eq. (5) reads

$$H_{U,RL}(t) = w(t) \int \frac{dk}{2\pi}\frac{dk'}{2\pi} [B_{k'}^\dagger B_k]_{10} U_{k-k'} c_{k'R}^\dagger c_{kL} + \text{H.c.}, \tag{6}$$

where $[M]_{10}$ denotes the off-diagonal component of the 2×2 matrix M. Equation (6) gives rise to a nonzero backscattering current operator $\delta I(t) = -\frac{1}{2} e d(N_R - N_L)/dt$. We evaluate the average backscattering current $\langle \delta I(t) \rangle$ using the Kubo formula [31], treating $H_{U,RL}$ as a time-dependent perturbation. We find

$$\langle \delta I(t) \rangle = e \int \frac{dk}{2\pi}\frac{dk'}{2\pi} |[B_{k'}^\dagger B_k]_{10}|^2 |U_{k-k'}|^2 (f_{-kL} - f_{kR}) \times 2\text{Re} \int_{-\infty}^0 dt' e^{-i(vk+vk'+i0)t'} w(t) w(t'+t). \tag{7}$$

Here, we introduced Fermi functions $f_{k\alpha} = f(\alpha vk - \mu_\alpha) = \langle c_{k\alpha}^\dagger c_{k\alpha} \rangle$ with $f(E) = (e^{E/T}+1)^{-1}$; we identify here $R \equiv +$ and $L \equiv -$. Treating backscattering as a weak perturbation, we use unperturbed Fermi functions where the bias voltage V is incorporated by setting chemical potentials $\mu_{R,L} = \mu \pm \frac{1}{2} eV$ for right and left movers. As a sanity check, static perturbations with $w(t) =$ constant impose $k = -k'$, and thus, $[B_{k'}^\dagger B_k]_{10} = 0$ in Eq. (7), implying that backscattering does not arise. We next take the linear-response limit $eV \ll T$, where $f_{-kL} - f_{kR} \approx f(vk-\mu)[1 - f(vk-\mu)]eV/T$.

The time-averaged backscattered current $\overline{\langle \delta I \rangle} = \mathcal{T}^{-1} \int_0^{\mathcal{T}} dt \langle \delta I(t) \rangle$ with $\mathcal{T} \to \infty$ is determined by the Fourier transform of the correlator $\overline{w(t)w(t'+t)}$. In terms of the power spectral density $S(\omega) = \int_{-\infty}^{\infty} dt' \times e^{i\omega t'} \overline{w(t)w(t'+t)}$, the correction to the dc conductance $\delta G = d\overline{\langle \delta I \rangle}/dV$ can be written as

$$\delta G = e^2 \int \frac{dk}{2\pi}\frac{dk'}{2\pi} |[B^\dagger_{k'+k_F} B_{k+k_F}]_{10}|^2 \times |U_{k+k'+2k_F}|^2 T^{-1} f(vk)[1-f(vk)] S(vk - vk'). \quad (8)$$

Since $S(\omega)$ is non-negative, the noise always decreases the dc edge conductance; i.e., $\delta G > 0$.

The integrals in Eq. (8) cannot be explicitly evaluated without specifying the function B_k that encodes the spin texture. However, tractable results can be obtained when the vector $\mathbf{d}_k$ specifying the texture via $B_k = \exp i\mathbf{d}_k \cdot \boldsymbol{\sigma}$ has a slowly varying magnitude d_k and a fixed direction $\mathbf{d}_k = d_k \hat{\mathbf{n}}$. The former assumption can be used in Eq. (8) to expand $[B^\dagger_{k'+k_F} B_{k+k_F}]_{10} \approx n_\perp v(k-k')/D_{k+k_F}$ with $n_\perp = [\hat{\mathbf{n}} \cdot \boldsymbol{\sigma}]_{10}$. Here, $D_{k+k_F} = v/\partial_k d_{k+k_F}$ defines the typical energy scale of the spin rotation (see Fig. 1). The expansion is valid when the noise spectrum is peaked at low frequencies so that $v(k-k') \ll D_{k+k_F}$ in the relevant region of integration in Eq. (8). Further assuming $v(k-k')$, $T \ll \mu$, we obtain

$$\delta G \approx \frac{G_0}{v^2} |U_{2k_F}|^2 n_\perp^2 D^{-2} \int \frac{d\omega}{2\pi} \omega^2 S(\omega), \quad (9)$$

where $D = D_{k_F}$. Equation (9) is valid for any μ/D. However, close to the Dirac point $k_F = 0$, the spin texture becomes quadratic (because of the property $d_k = d_{-k}$ following from time-reversal symmetry) with a curvature k_0^{-1}. When, $\max(\mu, T) \ll vk_0$, one can replace $D^{-1} \to \max(\mu, T)/(vk_0^2)$ in Eq. (9).

Telegraph noise from a charge puddle.—The conductance correction δG in Eq. (9) depends on the noise spectrum. A realistic source is telegraph noise caused by a charge puddle [20] with fluctuating charge. We model the puddle as a quantum dot that creates a local edge electric potential $W(x,t)$ dependent on the dot's configuration at a given time t. We assume that the dot has a sizable charging energy $E_C \gtrsim T$ so that only two charge states need to be retained. To simplify our description, we further ignore different states of the puddle within the same charge sector, which is justified if noise predominantly arises from electric dipole fluctuations contributed by different charge states. In this case, the puddle acts as a two-level system akin to a fluctuating dipole, [32] and its potential admits the separable form $W(x,t) = U(x)w(t)$ employed in Eq. (5). Here, $U(x)$ is the effective dipole potential (the difference in the potential in the two charge states), and $w(t)$ represents telegraph noise.

The charge puddle's classical noise spectrum is given by [33]

$$S(\omega) = p_0(1-p_0)\frac{2\tau}{1+\omega^2\tau^2}, \qquad (\omega \ll T), \quad (10)$$

where τ^{-1} is the relaxation rate of the excited state and p_0 is the probability for the TLS to be in its ground state. For a thermal population, we have $p_0 = 1/(1+e^{-\Delta/T})$ with $\Delta = 2E_C|\{N_g\} - \frac{1}{2}|$ the energy difference between the puddle's excited and ground states; $\{\ldots\}$ denotes the positive fractional part, while N_g is a dimensionless parameter determined by the puddle's electrostatic environment (e.g., a neighboring puddle) and thus varies between different TLSs. We treat N_g as a uniformly distributed random variable. Note, however, that N_g depends linearly on the edge chemical potential μ, which is tunable by a global gate. Therefore, due to the factor $p_0(1-p_0)$ in Eq. (10), we expect to see temperature-broadened resonances in δG of a short edge as the gate voltage is tuned; see Eq. (11) below. Gate-induced conductance fluctuations are consistent with experiments in existing 2D TI candidate materials [4,11,34].

The TLS noise spectrum Eq. (10) vanishes slowly at large frequencies $S(\omega) \sim 1/\omega^2$, resulting in a divergent integral (9) [35]. Our derivation of Eq. (9) starting from Eq. (5) treated the noise source w as classical, which restricts the validity of Eq. (9) to low frequencies, $\omega \ll T$. If the dominant contribution to the integral comes from higher frequencies, as is the case for the noise spectrum (10), one must use an equation that is valid also at higher frequencies. Such an equation is obtained from a proper quantum derivation that treats w as an operator, see Ref. [32]. Equation (9) generalized to higher frequencies is obtained by replacing $S(\omega) \to \{(\omega/2T)^2/[\sinh^2(\omega/2T)]\} S(\omega)$ in that equation. Using this quantum form in Eq. (9) yields

$$\delta G = G_0 \frac{2\pi}{3v^2} |U_{2k_F}|^2 n_\perp^2 \frac{T}{D^2\tau} p_0(1-p_0), \quad (11)$$

in the limit $\tau^{-1} \ll T$. This is the more refined version of Eq. (1) derived in the Introduction.

The temperature-dependence of Eq. (11) arises from three factors: the puddle occupation number p_0, the factor T coming from the sum over frequencies contributing to backscattering, and finally, from the so-far unspecified TLS relaxation rate τ^{-1}. The relaxation time is a sum of two microscopic times $\tau = \tau_{\rm esc} + \tau_{e-e}$: the time $\tau_{\rm esc}$ of elastic electron escape from the puddle and the inelastic energy relaxation time τ_{e-e}. The former is independent of temperature, while the latter for charge puddles varies as [22] $\tau_{e-e}^{-1} \propto T^2/\delta$ where δ is the puddle level spacing. At a temperature much higher than $\sqrt{\delta\tau_{\rm esc}^{-1}}$ one has $\tau_{e-e}^{-1} \gg \tau_{\rm esc}^{-1}$ so that $\tau^{-1} \approx \tau_{\rm esc}^{-1}$ is almost independent of temperature. The conductance correction Eq. (11) has then rather weak temperature dependence. We focus on this limit $\tau^{-1} \approx \tau_{\rm esc}^{-1}$ hereafter.

Long edge.—Equation (11) is valid for a single fluctuating TLS which is the relevant case for a short edge. Next, we consider the effects of multiple TLSs near the edge, which is appropriate for a long edge. The correction to conductance Eq. (11), due to a single TLS, can be translated into an added small resistance $\delta R = \delta G/G_0^2 \ll G_0^{-1}$ to the total edge resistance $R \approx G_0^{-1} + \delta R$. Assuming uncorrelated fluctuations of the TLSs, we can neglect interference contributions [36]; the resistance of a long edge is then $R \approx \sum_i \delta R_i$, where δR_i is the contribution from the ith TLS. Summing over i amounts to ensemble-averaging Eq. (11) over the random parameters, in particular, N_g. The average is dominated by those puddles where N_g is close to a half-integer $\Delta \ll T$. Interpreting τ^{-1} and $|U_{2k_F}|^2$ as their typical values at $\{N_g\} \approx 1/2$, we find therefore an edge resistance

$$R = LnG_0^{-1} \frac{\pi|U_{2k_F}|^2}{3v^2} n_\perp^2 \frac{T}{D^2\tau} \frac{T}{E_c} \tanh\frac{E_c}{2T}, \qquad (12)$$

where n is the one-dimensional impurity density [37] and L is the length of the edge. The factor $(2T/E_C)\tanh[E_c/(2T)] = 4\langle p_0(1-p_0)\rangle_{N_g}$ is the fraction of TLS for which $T \gg \Delta$. The noise time scale τ can be estimated by evaluating the escape rate of an electron from one charge puddle to a neighboring puddle [see comments below Eq. (11)]. Since $\{N_g\} \approx 1/2$, tunneling is resonant, and its rate is equal to the level splitting in the two-puddle problem. We can use the WKB approximation since the puddles are typically large [22]. This estimate gives $\tau^{-1} \sim \delta e^{-d/\Lambda}$, where δ is the puddle level spacing, Λ is the penetration depth of a low-energy electron into the bulk, and d is the average distance between the puddles. In the limit $T \gg E_c$, the resistance Eq. (12) is linear in temperature, while at low temperatures $R \propto T^2$. Strictly speaking, at $T \gg E_c$, one should include more charge states in our noise model. As long as $\tau^{-1} \ll E_c$, the puddle charge takes discrete well-defined values, and the noise has the Lorentzian form Eq. (10). The generalization of the prefactor $p_0(1-p_0)$ in that equation to many levels remains T independent at high temperatures.

$1/f$ noise.—Electronics ubiquitously exhibit $1/f$ noise. We therefore discuss the resulting resistance for this case, assuming that the noise source is extensive. Let us first discuss in which frequency range the noise from a collection of charge puddles can have a $1/f$ form. In Eq. (12), we took $\tau^{-1} \sim \delta e^{-d/\Lambda}$ with d the puddle-puddle distance. Assuming that the random variable d is distributed uniformly, the corresponding distribution of relaxation times $P(\tau) \sim 1/\tau$ is dominated by short times $\tau \sim 1/\delta$. Further assuming $\delta \ll T$, the resistance averaged over puddle positions then becomes

$$R \sim LnG_0^{-1} \frac{T\delta|U_{2k_F}|^2}{D^2 v^2} n_\perp^2 \qquad (13)$$

in the high-temperature limit $T \gg E_c$ while $R \propto T^2$ at $T \ll E_c$. By averaging Eq. (10) over τ with the distribution $1/\tau$, the resulting noise spectrum is $1/\omega$ at low frequencies $\omega \ll \delta$ but $1/\omega^2$ at high frequencies $\omega \gg \delta$. When $\delta \ll T$, the high-frequency part gives the dominant contribution to Eq. (13). This is because the transition matrix element becomes small at low energy transfers $[B^\dagger_{k'+k_F} B_{k+k_F}]_{10} \approx \delta/D$ when $v(k'-k) \approx \delta \ll D$; see discussion above Eq. (9).

Let us next discuss the more generic $1/f^\gamma$ noise without specifying its microscopic origin. For $1/f^\gamma$ noise $(0 < \gamma < 3)$ with a *sharp* high-frequency cutoff $\Omega \ll T$, we find $R \sim G_0^{-1}(\Omega/D)^2 n_\perp^2 S_0 |U_{2k_F}|^2/v^2$ with a γ-dependent numerical coefficient. This result is obtained from Eq. (8) by taking a spectrum $S(\omega) = |\omega|^{-\gamma}\Omega^{\gamma-1}S_0$, defined for $|\omega| < \Omega$.

Discussion.—The noise-induced backscattering underlying Eq. (8) relies on the presence of a momentum-space spin texture of the edge state. Although band theory predicts the existence of such a texture [38], its experimental detection is so far absent. As a simple experimental probe of the spin texture, we suggest creating a time-dependent "noise potential" artificially by an external gate; see Fig. 1(b). With ac voltage $V_0 \cos\omega_0 t$ applied to the gate, we have $U(x) = V_0 u(x)$ and $w(t) = \cos\omega_0 t$ in Eq. (5). The dimensionless function $u(x)$ is geometry dependent and can be, in principle found, by solving the Poisson equation. Using Eq. (9) with $S(\omega)$ obtained from w, we find in the limit ω_0, $T \ll D$, μ,

$$\delta G = G_0 \frac{\omega_0^2}{4D^2 v^2} V_0^2 |u_{2k_F}|^2 n_\perp^2. \qquad (14)$$

Remarkably, by the application of an ac gate voltage, one may create an effective backscattering potential $\propto \omega_0 V_0 u_{2k_F} n_\perp / D$ on the helical edge, as long as a spin texture exists. Quadratic dependence of δG on gate voltage and frequency thus constitutes a clear experimental signature of a spin texture in a helical edge. We note that for large $k_F = \mu/v$ it may be difficult in practice to create a sharp enough potential that induces substantial u_{2k_F}. This difficulty can be avoided if the Dirac point is not buried [12,39] and one can tune μ with a global gate to a smaller value. In this limit, there is an additional μ dependence in δG stemming from $D^{-2} \propto \mu^2$; see discussion below Eq. (9).

Let us finally estimate parameters of our noise models and discuss the size of the effect. For charge puddles, as was mentioned in the context of Eq. (13), the dominant contribution to resistance comes from close pairs of puddles for which $\tau^{-1} \approx \delta$. For HgTe, $\delta \approx \alpha^2 \Delta_b$ with $\alpha = e^2/4\pi\epsilon v$, and Δ_b is the band gap [40]. For a ball-park estimate of U_{2k_F}, we can use the charging energy $E_c \sim \alpha v/l$ of a charge puddle of size l, assuming a short-range potential then gives $U_{2k_F} \sim v\alpha$. Taking $n_\perp \sim 1$, we obtain the final estimate for the resistance in Eq. (13) $R \sim LnG_0^{-1}[(\alpha^4 T \Delta_b)/D^2]$. In HgTe, the interaction constant

$\alpha \approx 0.3$ is not very large, and near-edge puddles are possibly rare $n \sim 1/\mu$m. Therefore, in HgTe, fluctuating dipoles (modeled as TLSs) in the dielectric may give a larger source of resistance [32]. This contribution is $R \sim (1/G_0)[(LT)/v]\alpha N e^{-4d_0 k_F}(T^2/D^2)\tan\delta$, where N is the number of TLS in the dielectric, and $\tan\delta$ is its loss tangent; d_0 is the distance of the dielectric from the edge [41]. For example, a SiO_2 dielectric of size $2\times 2\times 0.1$ μm^3 ($L = 2$ μm) at temperature $T = 1$ K hosts [42] $N \sim 2\times 10^4$ contributing TLSs and has a loss tangent [43] $\tan\delta \sim 10^{-3}$. Assuming $T/D \sim 1$ and focusing on the vicinity of the Dirac point $k_F d_0 \lesssim 1$, the corresponding resistance is significant $R \sim G_0^{-1}$, even for a short $L = 2$ μm edge. For even shorter edges, the dominant contribution may come from gate noise; see Eq. (14).

Our main results, Eqs. (11) and (12), and the above estimates were derived for a specific model of a fluctuating dipole in thermal equilibrium. We emphasize that these results generalize to the case of a nonequilibrium noise source. An important example is when the effective noise temperature is much higher than the system temperature. The result for that case can be obtained by taking the high temperature limit in Eqs. (11) and (12).

The mechanism of noise-induced backscattering may play a role in broader settings in materials where elastic backscattering is suppressed, e.g., in graphene or in 3D topological insulators. Future studies of noise in such context may extend to topics such as spin relaxation [44] and dephasing of quasiparticle interference [45].

We thank Gijs de Lange and John Watson for helpful discussions and especially thank Leonid Glazman for his perceptive insights. We also gratefully acknowledge support from the National Science Foundation through Grant No. DMR-1723367; the Caltech Institute for Quantum Information and Matter, a NSF Physics Frontiers Center with support of the Gordon and Betty Moore Foundation through Grant No. GBMF1250; and the Walter Burke Institute for Theoretical Physics at Caltech.

[1] C. L. Kane and E. J. Mele, Phys. Rev. Lett. **95**, 146802 (2005).
[2] C. L. Kane and E. J. Mele, Phys. Rev. Lett. **95**, 226801 (2005).
[3] B. A. Bernevig and S.-C. Zhang, Phys. Rev Lett. **96**, 106802 (2006).
[4] M. König, S. Wiedmann, C. Brüne, A. Roth, H. Buhmann, L. W. Molenkamp, X.-L. Qi, and S.-C. Zhang, Science **318**, 766 (2007).
[5] A. Roth, C. Brüne, H. Buhmann, L. W. Molenkamp, J. Maciejko, X.-L. Qi, and S.-C. Zhang, Science **325**, 294 (2009).
[6] G. M. Gusev, Z. D. Kvon, E. B. Olshanetsky, A. D. Levin, Y. Krupko, J. C. Portal, N. N. Mikhailov, and S. A. Dvoretsky, Phys. Rev. B **89**, 125305 (2014).
[7] I. Knez, C. T. Rettner, S.-H. Yang, S. S. P. Parkin, L. Du, R.-R. Du, and G. Sullivan, Phys. Rev. Lett. **112**, 026602 (2014).
[8] L. Du, I. Knez, G. Sullivan, and R.-R. Du, Phys. Rev. Lett. **114**, 096802 (2015).
[9] F. Nichele, H. J. Suominen, M. Kjaergaard, C. M. Marcus, E. Sajadi, J. A. Folk, F. Qu, A. J. A. Beukman, F. K. de Vries, J. van Veen, S. Nadj-Perge, L. P. Kouwenhoven, B.-M. Nguyen, A. A. Kiselev, W. Yi, M. Sokolich, M. J. Manfra, E. M. Spanton, and K. A. Moler, New J. Phys. **18**, 083005 (2016).
[10] L. Du, T. Li, W. Lou, X. Wu, X. Liu, Z. Han, C. Zhang, G. Sullivan, A. Ikhlassi, K. Chang, and R.-R. Du, Phys. Rev. Lett. **119**, 056803 (2017).
[11] Z. Fei, T. Palomaki, S. Wu, W. Zhao, X. Cai, B. Sun, P. Nguyen, J. Finney, X. Xu, and D. H. Cobden, Nat. Phys. **13**, 677 (2017).
[12] S. Wu, V. Fatemi, Q. D. Gibson, K. Watanabe, T. Taniguchi, R. J. Cava, and P. Jarillo-Herrero, Science **359**, 76 (2018).
[13] C. Xu and J. E. Moore, Phys. Rev. B **73**, 045322 (2006).
[14] C. Wu, B. A. Bernevig, and S.-C. Zhang, Phys. Rev. Lett. **96**, 106401 (2006).
[15] J. Maciejko, C. Liu, Y. Oreg, X.-L. Qi, C. Wu, and S.-C. Zhang, Phys. Rev. Lett. **102**, 256803 (2009).
[16] Y. Tanaka, A. Furusaki, and K. A. Matveev, Phys. Rev. Lett. **106**, 236402 (2011).
[17] J. C. Budich, F. Dolcini, P. Recher, and B. Trauzettel, Phys. Rev. Lett. **108**, 086602 (2012).
[18] T. L. Schmidt, S. Rachel, F. von Oppen, and L. I. Glazman, Phys. Rev. Lett. **108**, 156402 (2012).
[19] V. Cheianov and L. I. Glazman, Phys. Rev. Lett. **110**, 206803 (2013).
[20] J. I. Väyrynen, M. Goldstein, and L. I. Glazman, Phys. Rev. Lett. **110**, 216402 (2013).
[21] B. L. Altshuler, I. L. Aleiner, and V. I. Yudson, Phys. Rev. Lett. **111**, 086401 (2013).
[22] J. I. Väyrynen, M. Goldstein, Y. Gefen, and L. I. Glazman, Phys. Rev. B **90**, 115309 (2014).
[23] N. Kainaris, I. V. Gornyi, S. T. Carr, and A. D. Mirlin, Phys. Rev. B **90**, 075118 (2014).
[24] Y.-Z. Chou, A. Levchenko, and M. S. Foster, Phys. Rev. Lett. **115**, 186404 (2015).
[25] The spin quantization can also be broken in a disordered manner; in this paper, we ignore these terms for simplicity. Note that they do not lead to significant backscattering at low temperature [26]. Electron-electron interactions together with the Rashba spin-orbit disorder lead to a correction to conductance that vanishes as T^4 (or with a higher power law) as $T \to 0$ [27].
[26] H.-Y. Xie, H. Li, Y.-Z. Chou, and M. S. Foster, Phys. Rev. Lett. **116**, 086603 (2016).
[27] M. Kharitonov, F. Geissler, and B. Trauzettel, Phys. Rev. B **96**, 155134 (2017).
[28] N. Lezmy, Y. Oreg, and M. Berkooz, Phys. Rev. B **85**, 235304 (2012).
[29] Localized spins may occur, e.g., due to charge puddles [20,22] or nuclear spins [30].
[30] C.-H. Hsu, P. Stano, J. Klinovaja, and D. Loss, Phys. Rev. B **96**, 081405 (2017); **97**, 125432 (2018).
[31] R. Kubo, J. Phys. Soc. Jpn. **12**, 570 (1957).

[32] See Supplementary Material at http://link.aps.org/supplemental/10.1103/PhysRevLett.121.106601, where we consider noise from fluctuating dipoles in the dielectric as well as a quantum mechanical treatment of $w(t)$.

[33] S. Kogan, *Electronic Noise and Fluctuations in Solids* (Cambridge University Press, Cambridge, England, 1996).

[34] T. Li, P. Wang, H. Fu, L. Du, K. A. Schreiber, X. Mu, X. Liu, G. Sullivan, G. A. Csáthy, X. Lin, and R.-R. Du, Phys. Rev. Lett. **115**, 136804 (2015).

[35] M. Toda, R. Kubo, R. Kubo, M. Toda, N. Saito, N. Hashitsume, and N. Hashitsume, *Statistical Physics II: Nonequilibrium Statistical Mechanics*, Springer Series in Solid-State Sciences (Springer, Berlin Heidelberg, 2012); D. Forster, *Hydrodynamic Fluctuations, Broken Symmetry, and Correlation Functions* (CRC Press, Boca Raton, FL, 1995).

[36] For example, in the case of two TLSs, of the form Eq. (6), the interference term will be proportional to $w_1(t)w_2(t+t')$, whose average over t is independent of t', and therefore, it does not contribute to $\langle\overline{\delta I}\rangle$ for the same reason as a static perturbation does not contribute to it.

[37] The density n is obtained from the two-dimensional density n_{2D} by multiplying the latter with the effective range ξ of the potential U; $n = n_{2D}\xi$. In practice, ξ is the screening length given by the distance to nearest gate.

[38] A. Rod, T. L. Schmidt, and S. Rachel, Phys. Rev. B **91**, 245112 (2015).

[39] R. Skolasinski, D. I. Pikulin, J. Alicea, and M. Wimmer, arXiv:1709.04830.

[40] From Ref. [22], we have $\delta \approx \alpha^2\Delta_b$ and $\alpha \approx 0.3$.

[41] For TLS in the bulk of the 2D TI, one can set $d_0 \to 0$ for TLS that are very close to the edge.

[42] R. B. Stephens, Phys. Rev. B **8**, 2896 (1973).

[43] M. Constantin, C. C. Yu, and J. M. Martinis, Phys. Rev. B **79**, 094520 (2009).

[44] J. H. Garcia, M. Vila, A. W. Cummings, and S. Roche, Chem. Soc. Rev. **47**, 3359 (2018).

[45] T. Zhang, P. Cheng, X. Chen, J.-F. Jia, X. Ma, K. He, L. Wang, H. Zhang, X. Dai, Z. Fang, X. Xie, and Q.-K. Xue, Phys. Rev. Lett. **103**, 266803 (2009); Z. Alpichshev, J. G. Analytis, J.-H. Chu, I. R. Fisher, Y. L. Chen, Z. X. Shen, A. Fang, and A. Kapitulnik, Phys. Rev. Lett. **104**, 016401 (2010).